*Indones. J. Chem., 2023, 23 (5), 1261 - 1269*

# Utilization of Steepest Ascent and Box-Behnken Design for Determination of Gadolinium in Acetonitrile by Differential Pulse Voltammetry

**Santhy Wyantuti*, Uji Pratomo, Yeni Wahyuni Hartati, Amelia Shafira,
Ari Hardianto, and Husein Hernandi Bahti**

*Department of Chemistry, Faculty of Mathematics and Natural Sciences, Universitas Padjadjaran,
Jl. Raya Bandung-Sumedang Km. 21, Jatinangor, Sumedang 45363, Indonesia*

* ***Corresponding author:***

*email: santhy.wyantuti@unpad.ac.id*

*Received: January 5, 2023*
*Accepted: September 5, 2023*

**DOI:** 10.22146/ijc.80979

***Abstract:*** *Gadolinium (Gd) is an important material for advanced technology; hence, the development of a sensitive and efficient alternative for the Gd-detection method to reduce the dependency on complicated and expensive methods has been massively investigated. Furthermore, the combination of differential pulse voltammetry (DPV) and the experimental design to detect Gd provides a simple, effective, and efficient method. In this study, the Steepest Ascent and Box-Behnken designs were chosen to determine the maximum voltammetry responses. The optimum conditions used for this study showed an amplitude modulation of 0.0884 V, potential deposition of 1.4382 V, and deposition time was 60.3615 s with the obtained recovery value, accuracy, and precision values being 98.37, 95.91, and 5.12% in relative standard deviation (RSD), respectively. Meanwhile, the detection and quantization limit values are 3.46 and 11.53 mg/L, respectively. Under optimum conditions, the presence of Gd in acetonitrile is determined in a mixture with Eu and Sm. Based on the results, the DPV method is capable of determining the presence of Gd in acetonitrile.*

***Keywords:*** *Gadolinium; differential pulse voltammetry; acetonitrile; Box–Behnken; Steepest Ascent*

## ■ INTRODUCTION

Gadolinium (Gd) belongs to the lanthanide group or rare earth elements that have great potential for the preparation of modern materials, specifically medical items [1-5]. Given that Gd has an important role in human welfare development, studies for the determination of its presence have significantly increased [6-7]. Furthermore, sophisticated methods such as inductively coupled plasma-mass spectrometry (ICP-MS) and inductively coupled plasma-atomic emission spectroscopy (ICP-AES) have shown great performance in determining the availability of Gd in samples, but they also have some drawbacks including complicated maintenance and high cost [8-10].

Voltammetry is one of the electrochemical methods used for measuring the current generated against the potential difference applied to the working electrode [11]. Advantages of the voltammetric method include a simple procedure, simultaneous analysis, and better detection limits [12-14]. An experimental design such as Steepest Ascent is a method used to detect the direction that the factor is moving to get the maximum response, while Box-Behnken design is used to estimate the interactions that occur to obtain an optimal process [15-16]. Determination of Gd using this method with Plackett-Burman and Box-Behnken experimental design has been carried out by using water solvent and $NH_4Cl$ electrolyte solution, but the voltammogram of rare earth elements' mixture is complicated as it has the same standard reduction potential value [17].

The demand for organic solvents for metal electrodeposition is increasing as it provides an alternative pathway for electrochemical processes as they accelerate the dissolution and reaction of metal ions [18-20]. In this study, the determination of Gd by differential pulse voltammetry (DPV) with acetonitrile as an organic solvent has been developed using the optimum factor determined by Steepest Ascent and Box-Behnken experimental designs to optimize the experiment time and reduce the chemicals used.

## ■ EXPERIMENTAL SECTION

### Materials

The materials used in this study were 65% nitric acid ($HNO_3$) and acetonitrile ($CH_3CN$), as well as aquabidest, which were obtained from Merck and aquamiliQ, respectively. The other reagents used were from Sigma Aldrich, which include 99% gadolinium oxide ($Gd_2O_3$), 99% dysprosium oxide ($Dy_2O_3$), 99.9% samarium oxide ($Sm_2O_3$), and 99.9% europium oxide ($Eu_2O_3$).

### Instrumentation

The apparatus and equipment used include scanning electron microscope (SEM) JEOL JSM-7500F, Ag/AgCl electrodes (eDAQ), ANOVA 7.0.0 program, potentiostat (Metrohm® µAutolab), Pt wire for the counter electrode (Antam), Minitab 17.1 program, analytical balance (Sartorius), and Pt working electrodes (Antam).

### Procedure

#### *Preparation of $Gd_2O_3$ stock solution 1000 mg/L*

The stock solution was made by dissolving 0.1153 g of $Gd_2O_3$ in 65% solution of $HNO_3$, which was stirred and boiled until a homogeneous solution was obtained, mixed with 100 mL of distilled water and stirred again. The solution was diluted with acetonitrile to produce varied amounts of Gd.

#### *Background current measurement*

A pipette was used to pour 10.0 mL of acetonitrile into a voltammetric cell. DPV was used to determine the current responsiveness of acetonitrile under the following conditions: a potential range, potential deposition, deposition time, amplitude modulation, and scanning rate of −1.0 to +1.0 V, −1.0 V, 60.0 s, 0.05 V, and 0.05 V/s, respectively.

#### *Gd current measurement*

DPV was used to determine the current response of a 30.0 mg/L $Gd_2O_3$ solution under the following conditions with potential range, deposition potential, deposition time, amplitude modulation, and scanning rate of −1.0 to +1.0 V, −1.0 V, 60.0 s, 0.05 V, and 0.05 V/s.

#### *Surface morphology analysis of Pt working electrode*

The surface morphology of the Pt working electrode (about 1 cm) was examined before and after deposition using SEM.

#### *Measurement of Gd with steepest ascent*

The selected upper and lower limit factors were set to measure Gd, namely the deposition potential of −1.0 and −2.0 V, deposition time of 40.0 and 80.0 s, and amplitude modulation of 0.05 and 0.10 V, then adjusted to the first-order model in the RStudio program [21-23] and the equation of the first-order model was used to determine the direction of the steepest ascent. The center was made along the direction of the experiment until the maximum response was generated, and then the experiment was designed. The result of Steepest Ascent optimization is shown in Table 1.

#### *Measurement of Gd with Box-Behnken design experimental design*

The current responses of 30 mg/L Gd were analyzed using differential pulse voltammetry for 45 measurements (3 repetitions) while Box-Behnken was used to optimize the selected factors with the lower and upper limits of steepest ascent experimental design results, namely the potential deposition of −1.4384 and

**Table 1.** Selected factors to be optimized by Steepest Ascent

| No | Potential deposition (V) | Deposition time (s) | Amplitude modulation (V) | Current (µA) |
|---|---|---|---|---|
| 1 | −1.4380 | 60.3300 | 0.0910 | 8.9326 |
| 2 | −1.4381 | 60.3362 | 0.0905 | 9.2975 |
| 3 | −1.4382 | 60.3462 | 0.0900 | 9.5924 |
| 4 | −1.4382 | 60.3489 | 0.0894 | 9.7140 |
| 5 | −1.4383 | 60.3552 | 0.0889 | 10.1540 |
| 6 | −1.4384 | 60.3615 | 0.0884 | 9.5479 |
| 7 | −1.4385 | 60.3678 | 0.0879 | 9.5768 |
| 8 | −1.4386 | 60.3741 | 0.0873 | 9.5768 |
| 9 | −1.4386 | 60.3804 | 0.0868 | 9.5321 |
| 10 | −1.4387 | 60.3867 | 0.0863 | 9.4800 |
| 11 | −1.4388 | 60.3931 | 0.0858 | 9.2071 |

**Table 2.** Selected factors to be optimized by Box-Behnken

| Factors | Level | | | Optimum condition |
|---|---|---|---|---|
| | −1 | 0 | +1 | |
| Potential deposition (V) | −1.4384 | −1.4383 | −1.4382 | −1.4382 |
| Deposition time (s) | 60.3489 | 60.3552 | 60.3615 | 60.3615 |
| Amplitude modulation (V) | 0.0894 | 0.0889 | 0.0884 | 0.0884 |

−1.4382 V, deposition time of 60.3489 and 60.3615 s, and amplitude modulation of 0.0894 and 0.0884 V. The data obtained were analyzed using the Minitab 19 program; the result of Box-Behnken optimization is shown in Table 2.

### *Determination of Gd in the REE mixture with Sm, Eu, and Dy*

A 10 mL of a combination of Sm, Eu, Gd, and Dy was pipetted in acetonitrile. Subsequently, the quantitative determination of the current was conducted by DPV under the Box-Behnken optimal condition.

### *Calibration curve of Gd*

A solution of 10.0, 20.0, 30.0, 40.0, and 50.0 mg/L Gd in acetonitrile were measured by DPV under the optimum condition obtained from Box-Behnken design.

## ■ RESULTS AND DISCUSSION

### The Acetonitrile and Gadolinium Current Response

The measurement of the acetonitrile current response was carried out to determine the effect of the solvent on the produced Gd response using the DPV method. As shown in Fig. 1, the acetonitrile did not produce any current response, while the 30 mg/L Gd in acetonitrile shows a characteristic peak near −0.40 V. From this preliminary result, the acetonitrile solvent does not interfere with the response of Gd.

### The Effect of Acetonitrile Concentration on the Gd Deposition on the Pt Electrode

Various concentration of Gd in acetonitrile (25, 75, and 100%) was deposited on the Pt electrode by the cyclic voltammetry method. The surface morphology before and after the electrodeposition was analyzed using SEM instrument, and the results obtained are shown in Fig. 2.

As shown in Fig. 2, the amount of Gd deposited on the Pt working electrode is indicated by the white particle aggregate. Furthermore, by increasing the concentration of acetonitrile, the aggregates were found to be highly distributed, and this indicates that an increase in the concentration of acetonitrile is proportional to the increase of white particle aggregate or deposition process of Gd on the working electrode of Pt.

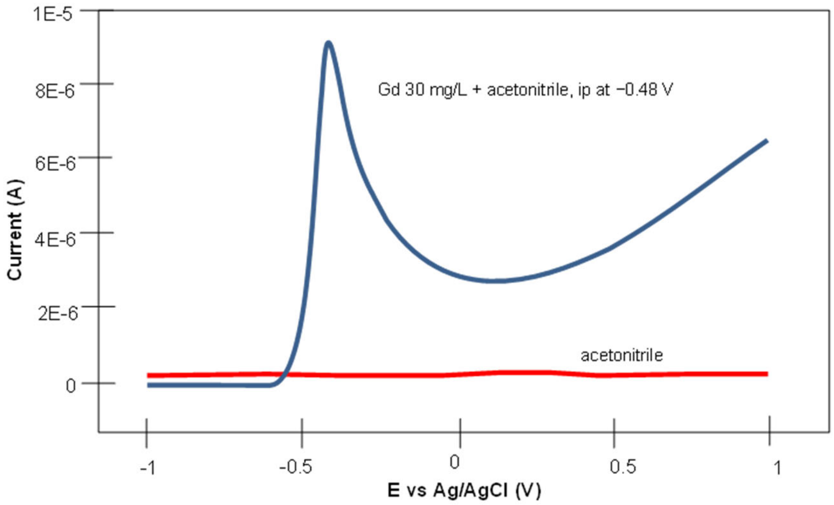

**Fig 1.** Current response of acetonitrile and Gd 30.0 mg/L in acetonitrile

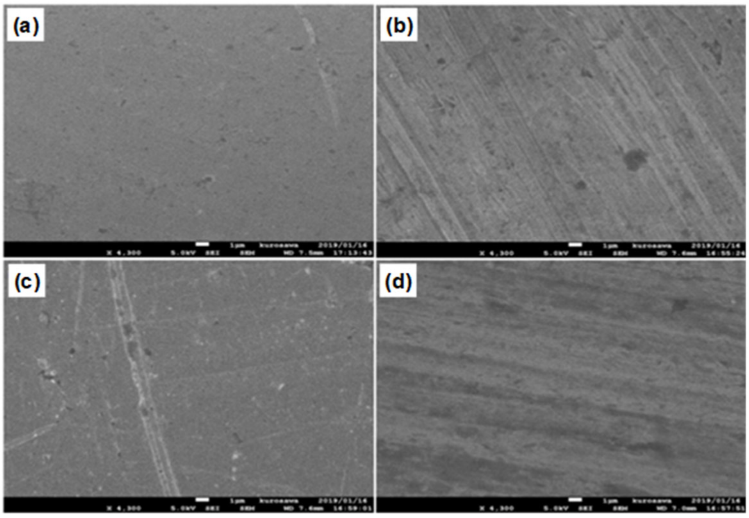

**Fig 2.** Pt electrode surface images (4300× magnification) after deposition of Gd in (a) 25% acetonitrile, (b) 75% acetonitrile, (c) 100% acetonitrile, and (d) before deposition

## Determination of the Optimum Condition with Box-Behnken Design

The main factors that considerably influence the optimum condition for Gd analysis are potential deposition, deposition time and amplitude modulation. They were optimized using Box-Behnken design in the Minitab 19 program. The three factors and three levels were selected, and the obtained current response is presented in Table 3.

The effect of the regression coefficient on the model is presented in Table 4. The *p*-value of the amplitude modulation factor is 0.0000 and less than 0.05; hence, the factor that significantly influences the measurement of current is amplitude modulation. Additionally, the *p*-values of deposition time and potential deposition are 0.8059 and 0.3784, and this indicates that deposition time and potential have no effect on the resulting response.

Furthermore, a fit test was carried out to determine

**Table 3.** The current response of Gd by DPV

| Run | Potential deposition (V) | Deposition time (s) | Amplitude modulation (V) | Current (μA) |
|---|---|---|---|---|
| 1 | −1.4384 | 60.3489 | 0.0889 | 11.5100; 11.1740; 11.3900 |
| 2 | −1.4382 | 60.3489 | 0.0889 | 11.7930; 10.9170; 11.2680 |
| 3 | −1.4384 | 60.3615 | 0.0889 | 11.7870; 11.3890; 11.3040 |
| 4 | −1.4382 | 60.3615 | 0.0889 | 11.8800; 11.6610; 11.0830 |
| 5 | −1.4384 | 60.3552 | 0.0884 | 10.9110; 10.9930; 10.7110 |
| 6 | −1.4382 | 60.3552 | 0.0884 | 10.4870; 10.8600; 10.9040 |
| 7 | −1.4384 | 60.3552 | 0.0894 | 10.8400; 10.8880; 10.5150 |
| 8 | −1.4382 | 60.3552 | 0.0894 | 10.1070; 10.5340; 10.3280 |
| 9 | −1.4383 | 60.3489 | 0.0884 | 10.7590; 10.1760; 10.4420 |
| 10 | −1.4383 | 60.3615 | 0.0884 | 10.6810; 10.6340; 10.4950 |
| 11 | −1.4383 | 60.3489 | 0.0894 | 9.9289; 9.9711; 9.9742 |
| 12 | −1.4383 | 60.3615 | 0.0894 | 9.8200; 9.7321; 9.6468 |
| 13 | −1.4383 | 60.3552 | 0.0889 | 9.2721; 9.3852; 9.2754 |
| 14 | −1.4383 | 60.3552 | 0.0889 | 9.8707; 9.8667; 9.6689 |
| 15 | −1.4383 | 60.3552 | 0.0889 | 9.5253; 9.6751; 9.3391 |

**Table 4.** Effect of the regression coefficient on the model

| Term | Coefficient | SE coefficient | *p* |
|---|---|---|---|
| Constant | 95.4210 | 0.0824 | 0.0000 |
| Deposition potential | −0.0450 | 0.0504 | 0.3784 |
| Deposition time | 0.0125 | 0.0504 | 0.8059 |
| Amplitude modulation | −0.2403 | 0.0504 | 0.0000 |
| Deposition potential*Deposition potential | 12.0750 | 0.0742 | 0.0000 |
| Deposition time* Deposition time | 0.7226 | 0.0742 | 0.0000 |
| Amplitude modulation*Amplitude modulation | −0.0764 | 0.0742 | 0.3108 |
| Deposition potential*Deposition time | −0.0225 | 0.0713 | 0.7543 |

whether the model agrees with the prediction model. The obtained *p*-value is 0.0413, which was lower than $\alpha = 0.05$ and this indicated that the model is appropriate.

Additionally, it is necessary to test for normality by observing the residual distribution curve. According to the hypothesis for the normality test, when $H_0$ is accepted at a *p*-value ≥ 0.05, it shows that the result is normally distributed. Meanwhile, when $H_1$ is accepted at a *p*-value less than 0.05, it shows that the result is not normally distributed. As illustrated in Fig. 3, the normal distribution curve of the hypothetical residual has a *p*-value above 0.05. Therefore, when $H_0$ is accepted shows that the residuals were normally distributed and significant. The best conditions for Gd detection include a potential deposition, deposition time, and amplitude modulation of −1.4382 V, 60.3615 s, and 0.0884 V, respectively.

## Detection of Gd in a Mixture with Sm, Eu, and Dy under the Optimum Condition

The concentration of Sm, Eu, Gd, and Dy in naturally occurring monazite on Bangka Belitung Island was 40.21, 0.01, 0.58, and 0.37%, respectively [14,24]. Therefore, various concentrations of Sm, Eu, Gd, and Dy were prepared in this study at 400, 1, 50, and 30 mg/L, respectively. The results are presented in Fig. 4.

Fig. 4 shows that the voltammogram relatively shows no response to the individual Eu and Sm in acetonitrile. Meanwhile, the presence of Gd and Dy produces a high and low current response, respectively. The voltammogram analysis of the mixture of Gd, Eu, Dy, and Sm showed a high current peak at ip −0.70 V, which resembles the peak of Gd at −0.48 V.

In addition, investigation on the mixtures of 50 mg/L Gd with 30 mg/L Dy, 50 mg/L Gd with 1 mg/L Eu, and 50 mg/L Gd with 400 mg/L Sm were carried out, and the result is presented in Fig. 5. Fig. 5(a) shows that a low current response of Dy in acetonitrile is observed while a relatively high current response of Gd is observed. Also, the mixture of Gd and Dy in acetonitrile shows a similar response with a higher response to Gd

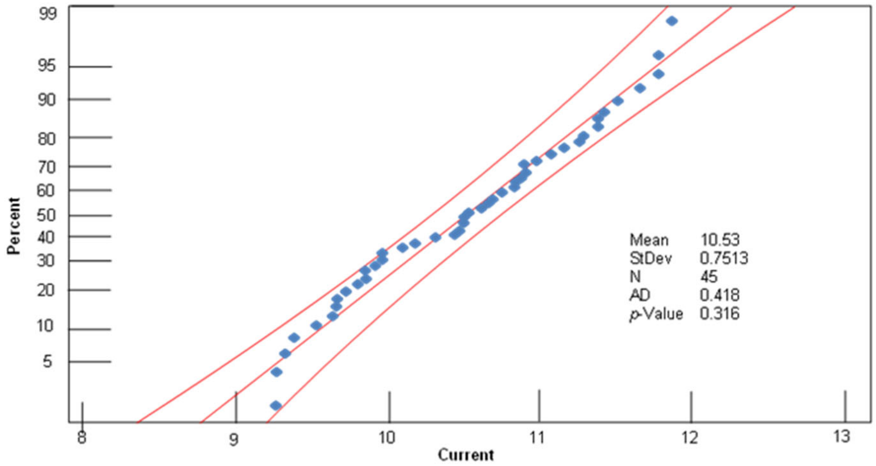

**Fig 3.** Normality plot of Box-Behnken design

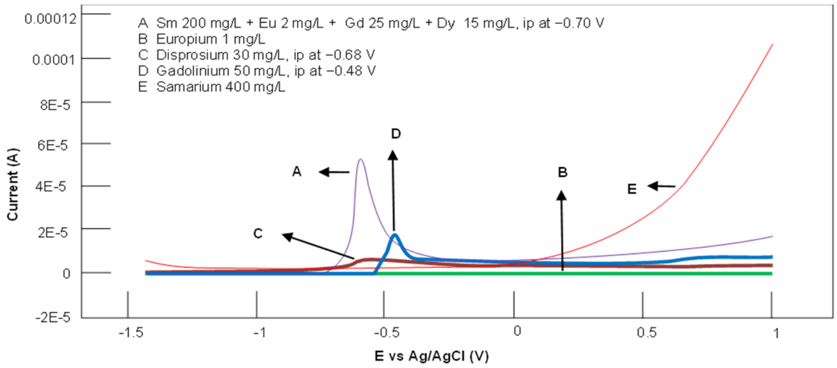

**Fig 4.** The individual current response of Gd 50 mg/L, Eu 1 mg/L, Dy 30 mg/L, and Sm 400 mg/L, and the mixture of Gd, Dy, Eu and Sm under the optimum conditions by DPV

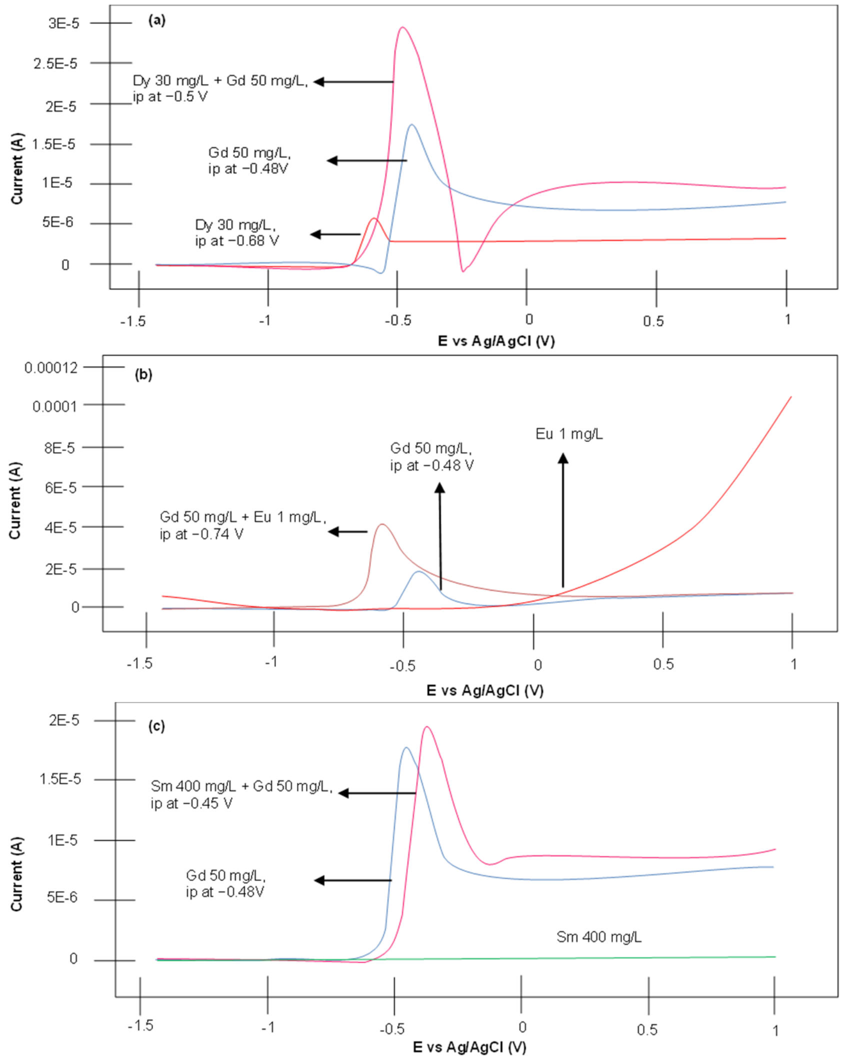

**Fig 5.** Voltammogram of (a) a mixture of Gd 50 mg/L and Dy 30 mg/L, (b) a mixture of Gd 5 mg/L and Eu 1 mg/L, and (c) a mixture of Gd 50 mg/L and Sm 400 mg/L under the optimum conditions by DPV

peak. In contrast, the voltammogram of individual Eu (Fig. 5(b)) and individual Sm (Fig. 5(c)) in acetonitrile shows no current response; however, the mixture of Gd-Eu and Gd-Sm shows a similar current response to individual Gd peak. Conclusively, this result indicates that Gd is determinable in a mixture of Sm and Eu.

## The Gd Calibration Curves, Detection Limits, and Quantification Limits

The Gd calibration curve was plotted at several concentrations, including 10, 20, 30, 40, and 50 mg/L. Fig. 6 and 7 depict the current response and the calibration curve, respectively. The differential pulse voltammetry current response demonstrates that the growing current peak is proportionate to the increasing Gd concentration. The graph of current was plotted with a coefficient ($R^2$) of 0.9995.

The precision, detection, and quantitation limit of the analytical parameters were determined to validate the level of acceptance and significance of the technique in the analysis. The average accuracy and precision were 95.91 and 5.12% (RSD), respectively, while the detection and quantitation limits were 3.46 and 11.53 mg/L, respectively, and the recovery (%R) calculation was 98.37%. In addition, the comparison between the previous work and this work is shown in Table 5. This research shows better recovery results for the determination of Gd by DPV method.

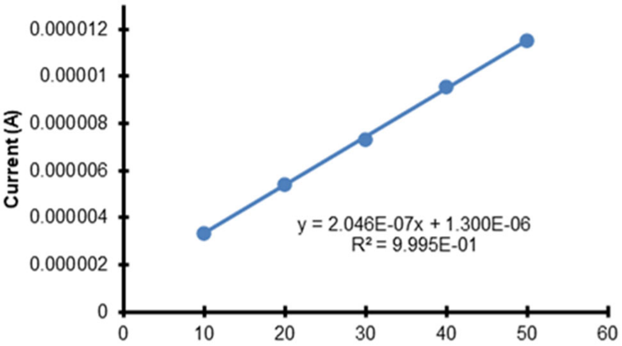

**Fig 7.** Calibration curve of Gd in acetonitrile under potential range −1.4382 to +1.0 V, potential deposition −1.4382 V, deposition time 60.3615 s, amplitude modulation 0.0884 V and scan rate 0, 05 V/s

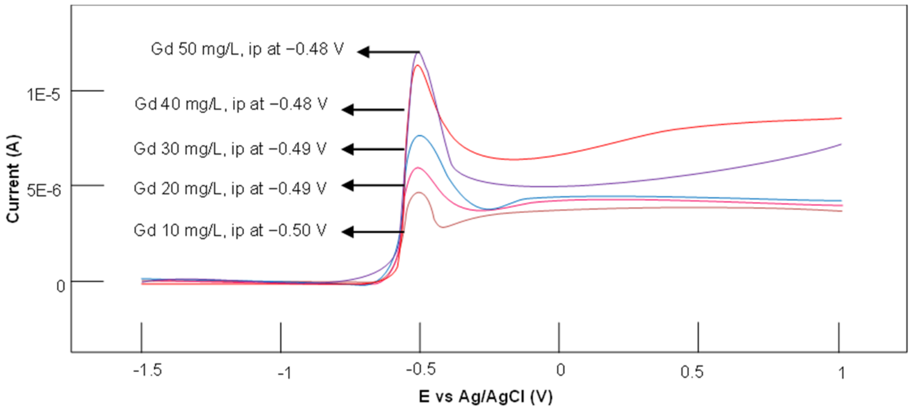

**Fig 6.** DPV of Gd in acetonitrile 10 to 50 mg/L under the potential range of −1.4382 to +1.0 V, deposition potential −1.4382 V, deposition time 60.3615 s, amplitude modulation 0.0884 V and scan rate 0.05 V/s

**Table 5.** Result comparison with the previous work

| Method | Solvent | % Recovery | Reference |
|---|---|---|---|
| Determination of Sm as a complex with DTPA by DPV based on Plackett-Burman experimental design | $NH_4Cl$ | 95.754 | [11] |
| Determination of Gd and Tb as complexes with DTPA by DPV based on Plackett-Burman experimental design | $NH_4Cl$ | 95.754 | [23] |
| Determination of Dy by DPV based on the Box-Behnken experimental design | $CH_3CN$ | 93.620 | [14] |
| Determination of Sm by DPV based on the Box–Behnken experimental design | $CH_3CN$ | 98.070 | [24] |

| Method | Solvent | % Recovery | Reference |
|---|---|---|---|
| Determination of Gd by DPV based on the Steepest Ascent and Box-Behnken experimental design | $CH_3CN$ | 98.375 | This research |

## CONCLUSION

The optimum measurement conditions for the detection of Gd in acetonitrile obtained from the Steepest Ascent experimental design and Box-Behnken are potential deposition of –1.4382 V, amplitude modulation of 0.0884 V, and deposition time of 60.3615 s. The recovery value, accuracy and precision were 98.37, 95.91, and 5.12% (RSD), respectively, while the LoD and LoQ obtained were 3.46 and 11.53 mg/L. Based on the results, the differential pulse voltammetry is usable in determining the presence of Gd in acetonitrile. Our research provides essential information for the further development of the Gd detection method from rare earth sources like monazite, which has a complex sample matrix potentially interfering with measurement.

## ACKNOWLEDGMENTS

The author would like to acknowledge the financial support from the Academic Leadership Grant Program, Padjadjaran University, the Directorate of Research and Community Service through *Riset Kompetensi Dosen Unpad* (DRPM-RKDU), Padjadjaran University, Indonesia [1549/UN6.3.1/PT.00/2023].

## AUTHOR CONTRIBUTIONS

The conceptualization, methodology, supervision, project administration, funding acquisition and resources were prepared by Santhy Wyantuti, Yeni Wahyuni Hartati, Uji Pratomo, and Husein Hernandi Bahti. The software, validation, writing–original draft preparation, and writing–review were done by Santhy Wyantuti, Uji Pratomo, Yeni Wahyuni Hartati, Ari Hardianto, and Husein Hernandi Bahti. The formal analysis, investigation, data curation, and visualization were done by Amelia Shafira, and Ari Hardianto. All authors have read and agreed to the published version of the manuscript.

## REFERENCES

[1] Unruh, C., Van Bavel, N., Anikovskiy, M., and Prenner, E.J., 2020, Benefits and detriments of gadolinium from medical advances to health and ecological risks, *Molecules*, 25 (23), 5762.

[2] Zhou, B., Li, Z., and Chen, C., 2017, Global potential of rare earth resources and rare earth demand from clean technologies, *Minerals*, 7 (11), 203.

[3] Yan, D., Ro, S., Sunam, O., and Kim, S., 2020, On the global rare earth elements utilization and its supply-demand in the future, *IOP Conf. Ser.: Earth Environ.*, 508, 012084.

[4] Blomqvist, L., Nordberg, G.F., Nurchi, V.M., and Aaseth, J.O., 2022, Gadolinium in medical imaging-usefulness, toxic reactions and possible countermeasures-A review, *Biomolecules*, 12 (6), 742.

[5] Kim, H.K., Lee, G.H., and Chang, Y., 2018, Gadolinium as an MRI contrast agent, *Future Med. Chem.*, 10 (6), 639–661.

[6] Veiga, M., Mattiazzi, P., de Gois, J.S., Nascimento, P.C., Borges, D.L.G., and Bohrer, D., 2020, Presence of other rare earth metals in gadolinium-based contrast agents, *Talanta*, 216, 120940.

[7] Smoliński, A., Stempin, M., and Howaniec, N., 2016, Determination of rare earth elements in combustion ashes from selected Polish coal mines by wavelength dispersive X-ray fluorescence spectrometry, *Spectrochim. Acta, Part B*, 116, 63–74.

[8] Zawisza, B., Pytlakowska, K., Feist, B., Polowniak, M., Kita, A., and Sitko, R., 2011, Determination of rare earth elements by spectroscopic techniques: A review, *J. Anal. At. Spectrom.*, 26 (12), 2373–2390.

[9] Telgmann, L., Lindner, U., Lingott, J., and Jakubowski, N., 2016, Analysis and speciation of lanthanoides by ICP-MS, *Phys. Sci. Rev.*, 1 (11), 20160058.

[10] Day, P., Erdahl, S., Eckdahl, S., Bornhorst, J., and Jannetto, P.J., 2019, Gadolinium-based contrast agents: A clinically significant analytical interference in inductively coupled plasma mass spectrometry elemental analysis, *Ann. Clin. Biochem.*, 56 (6), 638–645.

[11] Wyantuti, S., Pratomo, U., Hartati, Y.W., Hendrati, D., and Bahti, H.H., 2018, A study of green electro-analysis conducted by experimental design method for detection of samarium as complex with diethylenetriaminepentaacetic acid (DTPA), *AIP Conf. Proc.*, 2049, 030010.

[12] Scholz, F., 2015, Voltammetric techniques of analysis: The essentials, *ChemTexts*, 1 (4), 17.

[13] Han, H., and Pan, D.J., 2021, Voltammetric methods for speciation analysis of trace metals in natural waters, *Trends Environ. Anal. Chem.*, 29, e00119.

[14] Wyantuti, S., Pratomo, U., Shauvina, S., Hartati, Y.W., and Bahti, H.H., 2021, Differential pulse voltammetry study for quantitative determination of dysprosium(III) in acetonitrile solution, *Int. J. Renewable Energy Dev.*, 10 (2), 191–199.

[15] Yu, X.L., and He, Y., 2017, Application of Box-Behnken designs in parameters optimization of differential pulse anodic stripping voltammetry for lead(II) determination in two electrolytes, *Sci. Rep.*, 7 (1), 2789.

[16] Liu, J., Xu, Y., Liu, S., Yu, S., Yu, Z., and Low, S.S., 2022, Application and progress of chemometrics in voltammetric biosensing, *Biosensors*, 12 (7), 494.

[17] Wyantuti, S., Harahap, F.W., Hartati, Y.W., and Firdaus, M.L., 2021, Application of Plackett-Burman and Box-Behnken experiment design in differential voltammetry analysis for determining gadolinium concentration, *J. Phys.: Conf. Ser.*, 1731, 012017.

[18] Neuróhr, K., Pogány, L., Tóth, B., Révész, A., Bakonyi, I., and Péter, L., 2017, Electrodeposition of Ni from various non-aqueous media: The case of alcoholic solutions, *J. Electrochem. Soc.*, 162, D256.

[19] Bourbos, E., Giannopoulou, I., Karantonis, A., Paspaliaris, I., and Panias, D., 2018, Reduction of light rare earths and a proposed process for Nd electrorecovery based on ionic liquids, *J. Sustainable Metall.*, 4 (3), 395–406.

[20] Mirzamohammadi, S., Khorsand, H., and Aliofkhazraei, M., 2017, Effect of different organic solvents on electrodeposition and wear behavior of Ni-alumina nanocomposite coatings, *Surf. Coat. Technol.*, 313, 202–213.

[21] Joyce, A.P., and Leung, S.S., 2013, Use of response surface methods and path of steepest ascent to optimize ligand-binding assay sensitivity, *J. Immunol. Methods*, 392 (1), 12–23.

[22] Jalalvand, A.R., 2022, Engagement of chemometrics and analytical electrochemistry for clinical purposes: A review, *Chemom. Intell. Lab. Syst.*, 227, 104612.

[23] Wyantuti, S., Pratomo, U., Hartati, Y.W., Hendrati, D., and Bahti, H.H., 2019, Application of experimental design by differential pulse voltammetry for determination of rare elements as complexes with diethylenetriaminepentaacetic acid (DTPA), *Int. J. Recent Technol. Eng.*, 8 (2S7), 33–37.

[24] Wyantuti, S., Pratomo, U., Manullang, L.A., Hendrati, D., Hartati, Y.W., and Bahti, H.H., 2021, Development of differential pulse voltammetric method for determining samarium(III) through electroanalytical study of the metal ion in acetonitrile using Box–Behnken design, *Heliyon*, 7 (4), e06602.